Optical studies of Pb^{2+} ions in a $LiBaF_3$ crystal

2006 J. Phys.: Condens. Matter 18 4985

(http://iopscience.iop.org/0953-8984/18/20/021)

INSTITUTE OF PHYSICS PUBLISHING JOURNAL OF PHYSICS: CONDENSED MATTER

J. Phys.: Condens. Matter **18** (2006) 4985–4993 doi:10.1088/0953-8984/18/20/021

Optical studies of Pb^{2+} ions in a $LiBaF_3$ crystal

L K Aminov, S I Nikitin, N I Silkin[1], A A Shakhov, R V Yusupov, R Yu Abdulsabirov and S L Korableva

Kazan State University, Kremlevskaya 18, 420008 Kazan, Russia

E-mail: Nikolai.Silkin@ksu.ru

Received 6 January 2006
Published 5 May 2006
Online at stacks.iop.org/JPhysCM/18/4985

Abstract

The absorption and luminescence spectra of a $LiBaF_3$:Pb^{2+} crystal are studied in the temperature range 10–300 K. At 300 K a structureless absorption band (A band) is found in the energy range 1.4–6.6 eV. The luminescence spectra at 300 and 10 K are composed of two A′ and A_1 bands with maxima at ∼5.0 and ∼4.0 eV, respectively. The A′ band originates from the 'regular' Pb^{2+} centres. The A′ band luminescence decay is single-exponential in the whole temperature range 10–300 K. The properties of the observed absorption and A′ luminescence bands are described well within the semiclassical theory based on the Franck–Condon principle and the Jahn–Teller effect in the excited sp configuration. The possible nature of the A_1 band luminescence is discussed.

1. Introduction

Ionic crystals doped with ns^2-ions such as Tl^+, Pb^{2+}, and Bi^{3+} have been studied for several decades. These compounds reveal a wide range of luminescent properties and are interesting as promising materials for scintillators and solid-state UV lasers.

A great amount of data on ns^2-ions in alkali halides can be found in the literature (see reviews [1, 2]). The properties of such ions in alkaline-earth fluorides have also been well studied [3–5]. In the former crystals the ns^2-ions are located in the anionic octahedron while in the latter they are found in a cubic 8-fold surrounding. Our interest concerns fluoride crystals with the perovskite structure, where ns^2-ions are located in a 12-fold fluorine surrounding. Previously, we have studied the absorption and luminescence of Tl^+ ions in $KZnF_3$ and $KMgF_3$ crystals [6, 7]. In spite of the great similarity of the host lattices the luminescent properties of these crystals differ significantly.

The subject of this paper is the study of the luminescent properties of the $LiBaF_3$:Pb^{2+} system. The $LiBaF_3$ crystal has an inverted perovskite structure (figure 1) with the divalent barium ion found in a cubic 12-fold fluorine surrounding, in contrast to the conventional fluoroperovskites in which it is the monovalent cation that is 12-fold coordinated [8]. The

[1] Author to whom any correspondence should be addressed.

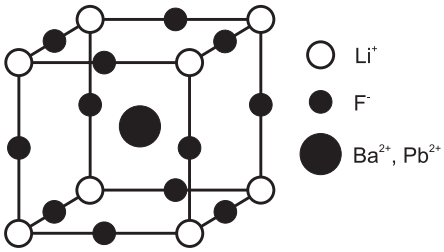

Figure 1. Unit cell of the $LiBaF_3$ crystal.

dopant Pb^{2+} ion has an ionic radius value ($R_i = 1.49$ Å) [9] close to that of the Ba^{2+} ion ($R_i = 1.61$ Å) and replaces it in the lattice.

Pure $LiBaF_3$, as well as Ce-doped and Rb-doped crystals, is a scintillator, enabling one to discriminate the thermal neutron and γ-radiations [10, 11]. It is a wide band-gap dielectric [12] and it might be a good host lattice for incorporating the ions with a lasing effect in the UV region.

During the last decade much effort has been put into spectroscopic studies of the radiation-induced defects of the nominally pure and Ce-doped $LiBaF_3$ crystal [13–15]. The structure and the luminescence of Ce^{3+}-centres in the $LiBaF_3$ crystal have also been a matter of intense research [16, 17]. An interesting transformation of Ce^{3+}-associated luminescence with temperature was observed and an unusual radiative de-excitation model involving Li–Ba cation exchange and Li_{Ba} antisite defects has been proposed [17].

At the same time, not much is known about the luminescence of the lead-doped $LiBaF_3$ compound. Compositions of $LiBa_{1-x}Pb_xF_3$ with x-values in the range 0–1 can be produced at least in a polycrystalline form [18]. The peak positions of the absorption and emission bands of Pb^{2+} ions in a number of fluoride hosts including $LiBaF_3$ were reported recently in [19] in connection with the possibility to sensitize a Gd^{3+}–Eu^{3+} downconversion ion pair. In [20] the luminescence of Pb^+ (1) centres in the $LiBaF_3$ crystal in the near-IR spectral region was studied. The energy of the absorption A band reported in [19] coincides well with the wavelength of the ArF excimer laser and together with the intense wide luminescence spectrum observed at room temperature this allows one to treat the $LiBaF_3$:Pb^{2+} crystal as a promising active medium for a tunable solid-state UV laser.

Within the frame of this work, pure and Pb^{2+}-doped $LiBaF_3$ single crystals were grown. Absorption and luminescence spectra as well as luminescence decay were studied in the temperature range 10–300 K. As the Pb^{2+} ion replaces the Ba^{2+} ion in the lattice there is no need for charge compensation, and the theory developed earlier [6, 7] to explain the luminescent properties of the $KZnF_3$:Tl^+ and $KMgF_3$:Tl^+ systems was readily applied to the $LiBaF_3$:Pb^{2+} crystal.

2. Experimental procedure

The $LiBaF_3$ crystals were grown from the melt in graphite crucibles at 850 °C by the Bridgman–Stockbarger method in a high-purity Ar atmosphere with a pressure of 1.5×10^5 Pa. The pulling rate was 1 mm h^{-1}. Dried LiF and BaF_2 compounds purified by recrystallization from the melt were used as the starting materials. The components were taken in the ratio of 60 mol% of LiF to 40 mol% of BaF_2 according to the phase diagram of the incongruently melted $LiBaF_3$ compound. Lead fluoride, PbF_2, was used to activate the crystals with Pb^{2+} ions. The Ar atmosphere was fluorinated by the gaseous products of Teflon pyrolysis in order to prevent

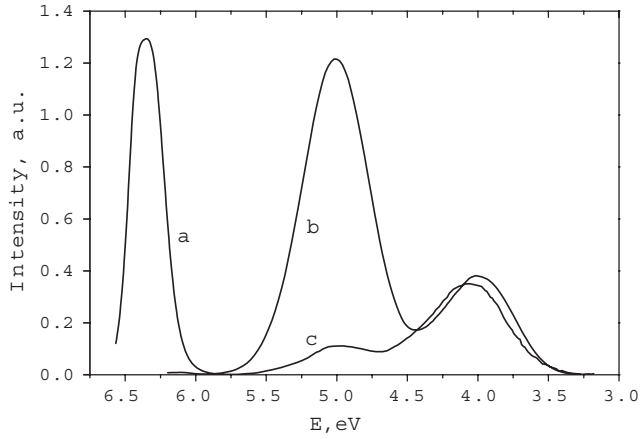

Figure 2. Absorption (a) and luminescence ((b), (c)) spectra of the $LiBaF_3$:Pb^{2+} crystals; for spectrum (b) the concentration of Pb^{2+} ions is ∼0.35 at.%, for spectrum (c) it is ∼0.03 at.%; $E_{exc} = 6.2$ eV, $T = 300$ K.

the reduction of the dopant PbF_2 [21] and to avoid the formation of centres containing O^{2-} or OH^- ions. In the current study crystals with concentration of PbF_2 in the initial melt of 0.15 and 2 at.% were used. The actual concentrations of Pb^{2+} ions in these crystals were found from the ratio of Pb to Ba x-ray induced luminescence intensities to be 0.03 and 0.35 at.%, respectively. These results confirm the segregation of Pb^{2+} dopant ions during the crystal growth reported in [21].

To evaluate the actual concentrations of lead in the grown crystals a Spectroscan x-ray fluorescence spectrometer was used.

The luminescence and excitation spectra were measured upon excitation with a DKsEl-1000 high-pressure xenon lamp with the use of an MDR-6 monochromator in the excitation channel and an MDR-23 monochromator in the registration channel. The measured spectra were not corrected to the spectral response. The absorption spectra were measured with a Specord M40 spectrophotometer.

The luminescence decay was studied upon excitation with a DKsSh-150 high-pressure xenon lamp operating in the pulse mode (the pulse duration being of about 30 ns). The luminescence was detected by a FEU-106 photomultiplier working in the photon counting mode (the 'dead time' of the registration system was 0.2 μs). For measurements in the temperature range 4.2–300 K an Oxford Instruments CF-1204 optical cryostat was used.

3. Experimental results

The absorption of ns^2-ions in crystals takes place usually in the UV region. Three absorption bands A, B and C corresponding to the transitions from the ground $|^1\Gamma_{1g}\rangle$ state to the excited $|^3\Gamma^*_{4u}\rangle$, $|^3\Gamma_{2u}\rangle$, $|^3\Gamma_{5u}\rangle$ and $|^1\Gamma^*_{4u}\rangle$ states originating from the electronic configuration nsnp are usually observed. Here $|^3\Gamma^*_{4u}\rangle$ and $|^1\Gamma^*_{4u}\rangle$ are the linear combinations of $|^3\Gamma_{4u}\rangle$ and $|^1\Gamma_{4u}\rangle$ states mixed by a strong spin–orbit interaction. Transitions $|^1\Gamma_{1g}\rangle \rightarrow |^3\Gamma^*_{4u}\rangle$ and $|^1\Gamma_{1g}\rangle \rightarrow |^1\Gamma^*_{4u}\rangle$ are thus allowed electric-dipole ones, resulting in a high oscillator strength of the corresponding absorption bands [2].

In the energy range 1.4–6.6 eV the studied $LiBaF_3$:Pb^{2+} crystals reveal an intense absorption band with $E_{max} = 6.34$ eV (A band) at $T = 300$ K (figure 2). In contrast to

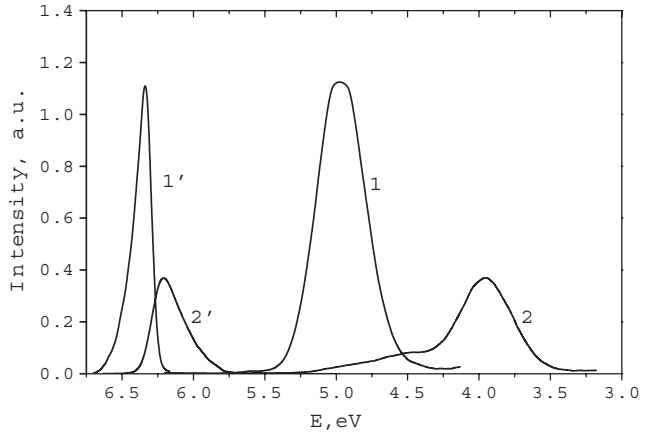

Figure 3. Luminescence A′ (1, $E_{exc} = 6.4$ eV) and A_1 (2, $E_{exc} = 6.2$ eV) bands of the $LiBaF_3$:Pb^{2+} crystal (0.35 at.% Pb^{2+} concentration) and the corresponding excitation spectra ($E_{reg} = 5.0$ eV, 1′ and $E_{reg} = 4.0$ eV, 2′, respectively), $T = 10$ K.

Tl^+ ions in $KZnF_3$ and $KMgF_3$ crystals, no doublet structure is found for this band. These results are fully in agreement with the data presented in [19].

Under the excitation to this band at $T = 300$ K the luminescence spectrum consists of two wide bands with maxima at 5.01 eV (A′) and 4.02 eV (A_1) and full widths at half maximum of 0.54 and 0.62 eV, respectively. In figure 2 the luminescence spectra of two samples with Pb^{2+} concentrations of 0.03 and 0.35 at.% are presented. It is clearly seen that the intensity of the A_1 band is almost the same for both crystals and the intensity of the A′ band follows strictly the concentration of the doped Pb^{2+} ions in the crystals. This allows us to assign the A′ band to Pb^{2+} ions.

With the temperature decrease no drastic changes of the luminescence spectrum are observed. At $T = 10$ K both A′ and A_1 bands remain structureless, with the maxima shifted to lower energies (4.98 and 3.96 eV, respectively) and full widths at half maximum decreased (0.40 and 0.37 eV, respectively; see figure 3). The integral intensity of the luminescence bands does not change in the temperature range 10–300 K. In figure 3 the excitation spectra of the A′ and A_1 bands at $T = 10$ K are also shown. These spectra differ in energy positions and bandshapes. At the same time, the excitation spectra of both bands are close in position to the A absorption band of Pb^{2+} ions.

The A′ band luminescence decay of the ns^2-ions in cubic surroundings has in general two components—fast and slow [1, 2, 7]. Our investigations have shown that the integral intensity of the fast luminescence is less than 1% of that for the slow one. In the temperature range 10–150 K the slow component of the A′ luminescence has a single-exponential character. Above 150 K its lifetime τ_s becomes shorter than 1 μs and this value is beyond the resolution of the experimental setup. The temperature dependence of the lifetime τ_s is shown in figure 4. To analyse this dependence the following expression, which is obtained by use of the conventional three-level model [1, 2, 7], was used:

$$\tau_s^{-1} = \frac{k_1 + gk_2 \exp(-\Delta E/k_B T)}{1 + g \exp(-\Delta E/k_B T)}, \tag{1}$$

where k_1 and k_2 are the probabilities of the radiative transitions from states 1 ($|^3\Gamma_{1u}\rangle$) and 2 ($|^3\Gamma^*_{4u}\rangle$), respectively, g is the ratio of their degeneracies ($g = 2$) and ΔE is the energy gap between these states (see figure 5). The convenience of this simplified expression is discussed

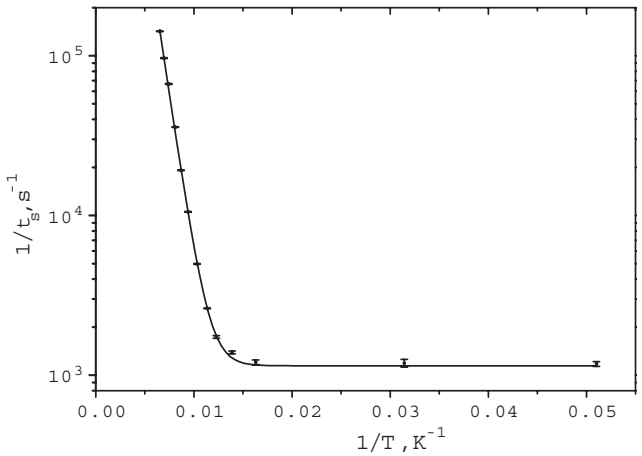

Figure 4. Temperature dependence of the A′ band luminescence lifetime τ_s (dots) and its fit to equation (1) (solid line).

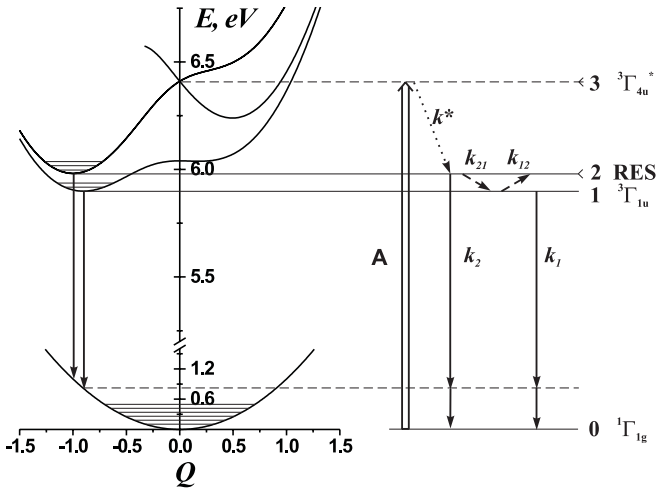

Figure 5. Cross-section of the adiabatic potential energy surfaces for the Pb^{2+} centre in the $LiBaF_3$ crystal, related to A absorption and A′ luminescence.

in the next section. The best-fit parameter values are:

$$k_1 = 1140 \pm 90\ s^{-1}, \qquad k_2 = (3.4 \pm 0.3) \times 10^7\ s^{-1}, \qquad \Delta E = 81 \pm 1\ meV. \tag{2}$$

4. Discussion

The most striking feature of the observed spectra of the $LiBaF_3$:Pb^{2+} crystal is the high value of the Stokes shift for the A′ band (1.33 eV) compared to its value for $KZnF_3$:Tl^+ (0.52 eV) and $KMgF_3$:Tl^+ (0.31 eV) crystals [7]. On the other hand, a similar situation was observed for the BaF_2:Pb^{2+} system (the Stokes shift is 1.27 eV) [5]. The direct consequence of such a high value of the Stokes shift is the absence of zero-phonon lines in the spectra at low temperatures.

To describe the absorption and luminescence spectra and the luminescence decay properties the semiclassical theory based on the Franck–Condon principle and the Jahn–Teller

effect for the excited sp configuration was used. This approach had been applied successfully to the $KZnF_3$:Tl^+ and $KMgF_3$:Tl^+ systems and was described in detail in [6, 7]. The model Hamiltonian is taken in the form typical for studies of optical centres formed by impurity s^2-ions, which occupy positions with cubic (or nearly cubic) symmetry in crystals:

$$H = H_0 + H_{ee} + H_{so} + H_{e-l}, \tag{3}$$

where H_0 corresponds to the single-electron approximation for a cubic quasi-molecule composed of a Pb^{2+} ion and its nearest surrounding, H_{ee} is the Coulomb repulsion of electrons, and H_{so} is the spin–orbit interaction. These three terms of the Hamiltonian result in the energy level pattern known as a Seitz scheme [22], with the ground $^1\Gamma_{1g}$ and two lowest excited $^3\Gamma_{1u}$ and $^3\Gamma^*_{4u}$ states. These states take part in the formation of the A absorption and the corresponding A′ luminescence bands. The transition $^1\Gamma_{1g} \leftrightarrow {}^3\Gamma^*_{4u}$ is known as an allowed electric-dipole one [1, 2]. Due to the spin–orbit interaction the $^3\Gamma^*_{4u}$ state is a mixture of Russel–Saunders terms with spins $S = 1$ and 0:

$$|^3\Gamma^*_{4u}\rangle = \mu|^3\Gamma_{4u}\rangle - \nu|^1\Gamma_{4u}\rangle \tag{4}$$

and the admixture of the $^1\Gamma_{4u}$ state higher in energy makes the transition allowed. The spin–orbit interaction in heavy $6s^2$-ions is rather strong, so the mixing of $^3\Gamma_{4u}$ and $^1\Gamma_{4u}$ states is essential. The degree of mixing is defined by the parameter $R = \mu^2/\nu^2$.

The term H_{e-l} includes the vibronic interaction and the elastic energy:

$$H_{e-l} = \sum V_i Q_i + \sum a_i Q_i^2. \tag{5}$$

Here Q_i are linear combinations of nuclear displacements from equilibrium positions (interaction modes), transforming in accordance with irreducible representations Γ_{1g} (Q_1), Γ_{3g} (Q_2, Q_3), Γ_{5g} (Q_3, Q_4, Q_5) of the cubic group O_h. The scale of Q_i is chosen in such a way that the elastic energy in the ground state has the form $\langle H_L\rangle_g = \sum Q_i^2$. For the excited configuration

$$H_L^{exc} = a_1 Q_1^2 + a_2(Q_2^2 + Q_3^2) + a_3(Q_4^2 + Q_5^2 + Q_6^2). \tag{6}$$

Coefficients a_1, a_2 and a_3 take into account the possible difference of effective elastic constants for the ground and excited configurations. The vibronic interaction term in equation (5) is treated in the same way as was done in [6, 7] and is described by the vibronic constants a, b and c for the interaction modes of Γ_{1g}, Γ_{3g} and Γ_{5g} symmetry for the triplet electronic states and a', b' and c' for singlet states, respectively.

Within the above approach we simulated the adiabatic potential energy surfaces (APESs) for the ground and excited states. This simulation should provide simultaneously the best fit to most of the experimental observables, namely, the energies of the absorption A and luminescence A′ bands, the shape of the absorption A band at $T = 300$ K, and the energy gap ΔE between the minima of the excited $^1\Gamma_{1g}$ and $^3\Gamma^*_{4u}$ states found from the luminescence decay studies. The shape of the A absorption band was obtained by a Monte Carlo simulation similar to that in [6]. Such an approach has allowed us to find the following set of the model parameters for the $LiBaF_3$:Pb^{2+} system:

$$\begin{aligned}
&a^2 = a'^2 = 0.25\ \text{eV}, \qquad b^2 = b'^2 = 0.01\ \text{eV},\\
&c^2 = 2.89\ \text{eV}, \qquad c'^2 = 4.30\ \text{eV},\\
&a_1 = a_2 = a_3 = 0.9, \qquad R = 8,\\
&E_1(^3\Gamma_{1u}) = 6.04\ \text{eV}, \qquad E_A = 6.41\ \text{eV},\\
&E_B = 7.85\ \text{eV}, \qquad E_C = 8.05\ \text{eV},\\
&\omega(\Gamma_1, \Gamma_3) = 200\ \text{cm}^{-1}, \qquad \omega(\Gamma_5) = 100\ \text{cm}^{-1}.
\end{aligned} \tag{7}$$

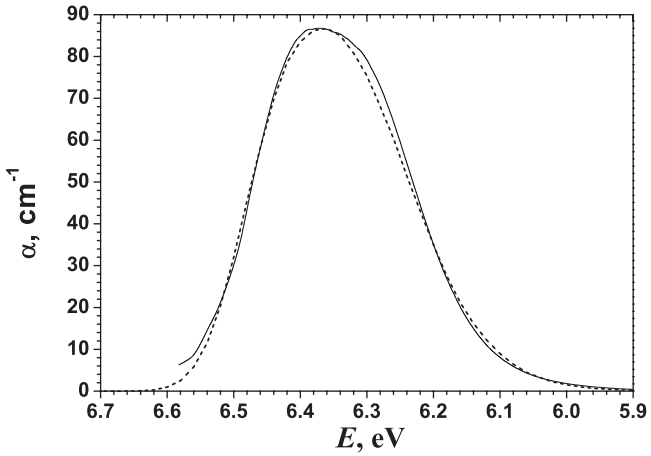

Figure 6. Absorption spectrum of the $LiBaF_3$:Pb^{2+} crystal with 0.03 at.% Pb^{2+} concentration at $T = 300$ K (solid line) and its Monte Carlo simulation (dashed line).

Here E_A, E_B, E_C are the energies of the A, B and C absorption bands taken from our measurements and the data of [19].

As was shown in [6, 7], in the case of the 12-fold surrounding the interaction with the vibrational modes of Γ_{5g} symmetry is predominant, and to a large extent it defines the observed spectral features. In the case of $LiBaF_3$:Pb^{2+} the corresponding parameters c and c' were found to be even greater. Also, compared to the data of [6, 7], the vibronic interaction with the totally symmetric mode Q_1 has increased more notably ($\sim$3 times).

The adiabatic potential pattern for the ground and the lowest excited states with the parameters (7) is shown in figure 5. The coordinate Q in figure 5 corresponds to the variation of the trigonal distortion in the $Q_4 = Q_5 = Q_6$ direction. Deep minima found both for $|^3\Gamma_{1u}\rangle$ and $|^3\Gamma^*_{4u}\rangle$ states at $Q \neq 0$ explain the high value of the Stokes shift. The presence of two minima, one nearly above the other, results in the 'red' shift of the maximum of the luminescence A′ band with the temperature decrease: at low temperatures practically all the transitions take place from the lower $|^3\Gamma_{1u}\rangle$ state. The absence of the zero-phonon line is also clear from figure 5. The value of $\Delta E = 82$ meV corresponds exactly to that found from the luminescence decay studies.

Figure 6 shows the result of the Monte Carlo simulation of the absorption A band for the Pb^{2+} ions in the $LiBaF_3$ crystal at $T = 300$. The simulated spectrum reproduces the experimental one quite well. The absence of the doublet structure typical for an ns^2-ion A absorption band is a consequence of the increased interaction with the totally symmetric Q_1 mode.

A relatively small value of the energy gap ΔE allows one to use the simple expression (1) to analyse the temperature dependence of the slow decay component of the A′ luminescence lifetime τ_s. This expression is suitable if the probability k_{21} of the nonradiative transitions between the states 1 and 2 is much higher than the probability of the radiative transition k_2 (see [7]). Such a relation between k_{21} and k_2 is clearly revealed by the fact that the intensity of the fast luminescence component is very low compared to that of the slow component. We note that this situation is again similar to that observed for BaF_2:Pb^{2+}, in which no fast luminescence was found [5]. Moreover, the probability k_{21} depends critically on the number of phonons involved in this nonradiative transition and thus on the value of ΔE. The value of ΔE can be

estimated rather well from the temperature dependence of the lifetime τ_s within the range in which it changes strongly. The value $\Delta E = 82$ meV was found to be even less than that for Tl^+ ions in the $KZnF_3$ crystal (147 meV, [7]). In the case of $KZnF_3$:Tl^+ the use of expression (1) was experimentally verified.

The value of $k_1 = 1140\ s^{-1}$ (see equation (2)) is much greater than that for Tl^+ ions in perovskites (86 s^{-1} for $KZnF_3$:Tl^+, 67 s^{-1} for $KMgF_3$:Tl^+ [7]). However, it is rather close to the value of k_1 in alkali halides (278 s^{-1} for KCl:Pb^{2+}, 909 s^{-1} for KBr:Pb^{2+} and 3570 s^{-1} for KI:Pb^{2+} [2]), in which the minimum of the metastable state is also shifted from the cubic symmetry position ($Q = 0$) and is close to that of the fast-radiating state (cf for instance [1]).

As far as the A_1 band luminescence is concerned, we may prove only that it is also due to an impurity-associated centre. Pure $LiBaF_3$ crystals do not show such a luminescence. Nevertheless, this luminescence is excited in the same wavelength region as the A′ band and reveals the same 'red' shift of the band maximum with the temperature decrease. Similar supplementary luminescence was found also for $KZnF_3$:Tl^+ [7] and $KMgF_3$:Tl^+ [23] crystals. Therefore we can presumably assign it to Pb^{2+} ions in a 'defect' crystalline site as well. A relatively high concentration of such defects in the $LiBaF_3$ crystal can arise due to the fact that contrary to the $KZnF_3$ and $KMgF_3$ crystals this compound is grown from a non-stoichiometric mixture of the initial components. Another possible explanation of the A_1 band is a perturbed exciton luminescence similar to the situation found for a number of Tl^+- and Pb^{2+}-doped caesium halides [24, 25]. The reason for this supposition is the fact that the A_1 luminescence band is observed in the energy region close to that of the luminescence of the self-trapped exciton in the pure $LiBaF_3$ crystal (4–4.2 eV) [10, 26, 13, 14]. Babin *et al* [19] also observed such a luminescence for a wide range of lead-doped fluorides and associated it with a host lattice.

Luminescence similar to the A_1 band was found to result from the Ce^{3+} ion electronic excitation in $LiBaF_3$:Ce^{3+} at temperatures higher than ∼150 K [17], in contrast to the low-temperature spectrum typical for Ce^{3+} centres. This observation has led the authors of [17] to the proposal of an unusual excited state structure with two types of minimum separated by an energy barrier and involving the so-called Li_{Ba} antisite defect. The latter is known as the most probable kind of the local charge compensation for Ce^{3+} centres. In the case of the $LiBaF_3$:Pb^{2+} crystal there is no necessity for charge compensation; therefore, this factor cannot result in the formation of such a defect.

5. Summary

The optical properties of the $LiBaF_3$:Pb^{2+} system with an inverted perovskite structure have been investigated in the energy range 1.4–6.6 eV.

(i) In this range an intense structureless absorption band with $E_{max} = 6.34$ eV (A band) is observed at $T = 300$ K.

(ii) Under excitation to the A band two wide luminescence bands with $E_{max} = 5.01$ eV (A′ band) and $E_{max} = 4.02$ eV (A_1 band) are observed at 300 K. At $T = 10$ K both bands remain structureless, with their maxima shifting to lower energies.

(iii) The positions and widths of the A absorption band and A′ luminescence band, the 'red' shift of the A′ band with temperature decrease, the lack of zero-phonon lines and the band structure are described well within the model developed earlier for ns^2-ions in perovskites. The origin of the A_1 luminescence band remains somewhat uncertain.

(iv) The differences in the optical properties of the $LiBaF_3$:Pb^{2+} crystal and the previously studied $KZnF_3$:Tl^+ and $KMgF_3$:Tl^+ crystals, namely, the high Stokes shift, greater width

and the absence of the doublet structure of the A absorption band, are most probably due to the increased vibronic interaction with the totally symmetric Q_1 and trigonal Q_4, Q_5 and Q_6 modes of the fluorine surrounding.

Acknowledgments

The authors are thankful to N G Ivoilov and I I Gil'mutdinov for the determination of the dopant concentration in grown crystals and to L V Mosina for help in preparation of the manuscript.

The work was supported by the Russian Foundation for Basic Research (project 03-02-17396), Research and Educational Center of Kazan State University (REC-007), the Regional Center for Collective Usage (RCCU) and the Ministry of Education and Science of the RF (project RNP 2.1.1.7348).

References

[1] Ranfagni A, Mugnai P, Bacci M, Viliani G and Fontana M P 1983 *Adv. Phys.* **32** 823
[2] Jacobs P W M 1991 *J. Phys. Chem. Solids* **52** 35
[3] Oboth K P, Lohmeier F J and Fischer F 1989 *Phys. Status Solidi* b **154** 789
[4] Overberg A and Fischer F 1988 *Phys. Status Solidi* b **147** 811
[5] Schotanus P, Van Eijk C W E, Blasse G and Den Hartog H W 1988 *Phys. Status Solidi* b **148** K77
[6] Aminov L K, Kosach A V, Nikitin S I, Silkin N I and Yusupov R V 2001 *J. Phys.: Condens. Matter* **13** 6247
[7] Aminov L K, Nikitin S I, Silkin N I, Shakhov A A and Yusupov R V 2002 *J. Phys.: Condens. Matter* **14** 13835
[8] Wyckoff R G 1948 *Crystal Structures* vol 2 (New York: Interscience)
[9] Shannon R D 1976 *Acta Crystallogr.* A **32** 751
[10] Knitel M J, Dorenbos P, De Haas J T M and Van Eijk C W E 1996 *Nucl. Instrum. Methods* A **374** 197
[11] Combes C M, Dorenbos P, Hollander R W and van Eijk C W E 1998 *Nucl. Instrum. Methods Phys. Res.* A **416** 364
[12] Bensalah A, Shimamura K, Fujita T, Sato H, Nikl M and Fukuda T 2003 *J. Alloys Compounds* **348** 258
[13] Tale I, Springis M, Rogulis U, Ogorodnik V, Kulis P, Tale V, Veispals A and Fitting H-J 2001 *Radiat. Meas.* **33** 751
[14] Tale I, Kulis P, Rogulis U, Tale V, Trokss J, Veispals A, Barboza-Flores M and Fitting H-J 1997 *J. Lumin.* **72–74** 722
[15] Rogulis U, Spaeth J-M, Tale I, Nikl M, Ichinose N and Shimamura K 2004 *Radiat. Meas.* **38** 663
[16] Yamaga M, Imai T, Shimamura K and Fukuda T 2001 *J. Cryst. Growth* **229** 487
[17] Nikl M, Mihókóva E, Málková Z, Vedda A, Martini M, Shimamura K and Fukuda T 2002 *Phys. Rev.* B **66** 184101
[18] Schmitz-Dumont O, Bergehoff I and Hartert E 1958 *Z. Anorg. Allg. Chem.* **283** 314
[19] Babin V, Oskam K D, Vergeer P and Meijerink A 2004 *Radiat. Meas.* **38** 767
[20] Prado L, Vieira N D Jr, Baldochi S L, Morato S P, Denis J P, Tercier N and Blanzat B 1996 *J. Chem. Phys. Solids* **57** 413
[21] Baldochi S L and Gesland J-Y 1992 *Mater. Res. Bull.* **27** 891
[22] Seitz F 1938 *J. Chem. Phys.* **6** 150
[23] Scacco A, Fioravanti S, Missori M, Grassano U M, Luci A, Palummo M, Giovenale E and Zema N 1993 *Phys. Chem. Solids* **54** 1035
[24] Aceves R, Babin V, Barboza Flores M, Fabeni P, Mihokova E, Nagirnyi V, Nikl M, Nitsch K, Pazzi G P, Perez Salas R and Zazubovich S 1998 *J. Phys.: Condens. Matter* **10** 5449
[25] Mihokova E, Nagirnyi V, Nikl M, Stolovich A, Pazzi G P, Zazubovich S and Zepelin V 1996 *J. Phys.: Condens. Matter* **8** 4301
[26] Shiran N V, Gektin A V, Voloshinovski A S and Voronova V V 1998 *Radiat. Meas.* **29** 295